LANGASITE RESONANT STRUCTURE: MICROMACHINING AND CHARACTERISATION

T. Leblois[(1)], O. Le Traon[(2)]

[(1)]MN2S Dept
Femto-ST Institute
University of Franche-Comte
Besançon, France
Therese.leblois@femto-st.fr

[(2)]DMPH/CMT
ONERA
Châtillon, France
Olivier.Le_Traon@onera.fr

ABSTRACT

This paper focuses on the micromachining of 3D microstructures on LGS plates by anisotropic wet etching. Several etching conditions are investigated to determine the best experimental way to fabricate 3D microstructures. The study covers the composition, the concentration and the temperature of the etching bath. Several types of experimental results are used to determine the conditions that provide consistent and reproducible results: the anisotropic factor, the etch rate and the degree of surface quality, the undercutting, the solution chemical aggressiveness toward masks. Etching profiles, SEM images are discussed on several orientations of etched plates. According to the experimental data base, an etchant is selected and the experimental conditions of etching are determined. 3D resonant structures are fabricated on the X cut using photolithographic process before the etching step. The final shapes of the structures are then characterized in view of inertial sensor design.

INTRODUCTION

Langasite (LGS) is suitable for generation of bulk and surface acoustic waves because of its high electromechanical coupling coefficient. So it can be considered as an alternative material to quartz crystal for acoustic wave (SAW, BAW) devices. In contrast to piezoelectric crystal like quartz or lithium niobate, langasite was shown to have piezoelectrically induced acoustic waves up to at least 1050°C. Hence, this material is very interesting for high temperature MEMS [1]. On the other hand, langasite is an interesting material for microbalance in liquid media and can be operated even in heavy viscosity liquids [2]. For vibrating inertial sensors such as vibrating beam accelerometers (VBA) [3] or Coriolis vibrating gyros (CVG) [4], langasite is also an attractive piezoelectric crystal in comparison with quartz, thanks to its potential high quality factor and higher electromechanical coupling, predicting an improvement of the bias stability and the signal to noise ratio of the sensors [5]. Several application areas of MEMS can be initiated with this material [6,7]. In all cases, the miniaturization of the structure is of prime importance. There is a lack of information on the anisotropy of LGS wet etching. Some studies [8] reported in the literature concern the polishing of some LGS plates. Recent works have shown that among acidic etchants specific to LGS, the HCl [7], H_2SO_4 [9] and H_3PO_4 [10] based solutions offer the advantage of etch rates comparable to those obtained by quartz. So the first part of this paper is focus on the characterization of the anisotropic dissolution process in several different solutions based on HCl acid. The etch rates and the changes in surface texture are determined. The second part is devoted to the micromachining of 3D microstructures (cantilevers, and tuning forks) in an X cut with the selected etching bath. The final shape of the structures and the underetching are characterized. These results demonstrate the feasibility of the micromachining by chemical etching of MEMS devices such as vibrating inertial sensors. Future works will be focus on the manufacturing of this kind of langasite devices.

CHARACTERISATION OF THE ANISOTROPIC CHEMICAL ATTACK OF LGS PLATES

Experimental details

Prior to the machining of micromechanical structures the etch behavior of langasite had to be investigated. Experiments with different crystal cuts show significantly varying etch rates. Thin circular plates were cut from a LGS ingot. 11 orientations (as defined in [11]) were selected (Table 1). The angles of cuts were determined using a double X-ray goniometer that offers an accuracy of about 30s. The faces were mechanically lapped. The commercial plates X, Y and Z come from VNISSIMS and FOMOS companies. The plates were etched at a constant temperature of 333K ±1K. Before and after etching, the variations of

thickness Δd were measured using a ''palmer'' instrument that provides an accuracy of about ± 1 µm. For LGS which belongs to class 32, the X axis is a two-fold axis and as a consequence the two faces of a Y$\pm\theta$ plate etch similarly. The etched rate is then given by the equation $R=\Delta d/2t$ where t is the etch duration. In the case of X cut, the equation gives an average value of the etched rate. Etched surfaces were examined by scanning electron microscopy or by interferometric microscopy. The surface roughness parameters Ra and Rq were determined by interferometric microscopy. The surface topography was also investigated using a mechanical profilometer. Several etching baths were investigated to highlight their more or less anisotropic properties. The solutions investigated here are based on HCl acid. The compositions of each solution are given in table 2. A comparison of the etch rates, surface roughness and anisotropy ratio is undertaken.

Experimental results

The first results concern the etch rates $R(\theta)$ calculated after an isothermal etching of 4 hours at 60°C. Variations of the etch rate as a function of the angles of cut θ are shown in Fig.1. Table 3 gives the etch rates R for the X cut.
Table 3 and Fig.1 reveal that:

(i) It is clear that the chemical etching in the four selected etchants is anisotropic. The Z cut is the cut that dissolves the more slowly which show a marked difference between quartz and LGS etching.

(ii) The evolutions of the etch rates versus θ are similar in the case of fluoride solutions. Nethertheless, HCl:HF solution dissolve twice as fast as the HCl:NH_4FHF bath. Curves C and D which are similar reveal higher values of etch rates. These last solutions are promising for chemical micromachining and deep etchings.

(iii) The anisotropic ratio which is determined by the equation Ar=Rmax/Rmin is maximal for the HCl:H_2O solution. This remark combined with very high dissolution rates makes this etchant very interesting for 3D micromachining.

Let us turn our attention to the degradation of the etched surfaces. For this purpose, surface textures are characterized and the roughness parameters are determined. Interferometric microscopic images of some deeply etched Y$\pm\theta$ plates and X cut are displayed in Fig.2 and Fig.3 respectively. These images call for a dissolution process governed by orientation. The dissolution figures which appear at the surface after etching clearly depend on the plates. We distinguish flat pits, elongated or bumpy hillocks and large hollows. Fig.4 shows the influence of etchants on the patterning of the surface. The geometrical features present on the surface may cause the decrease of the metrological performances of micro sensors. Some study showed a correlation between the roughness parameters and the metrological performances of resonant sensor. It is of major interest to reduce the surface roughness.

Table 1. Values of angles for the various cuts

Cut	X	Y	Z	Y$\pm\theta$
φ (°)	$\pm$ 90	0	0	0
θ (°)	0	0	$\pm$ 90	$\pm$ 20, $\pm$ 40, $\pm$ 60

Table 2. Composition of the four baths

Bath	HCl:HF	HCl:NH_4FHF	HCl:H_3PO_4	HCl:H_2O
Composition	4:3	4:3	1:1	2:1
Concentration	HCl (37%) HF(40%)	HCl (37%) NH_4FHF: 60g in 100ml DI water	HCl (37%) H_3PO_4 (85%)	HCl (37%)

Table 3. Values (in µm/h) of the etch rates R for X cut and the anisotropic factor Ar for the different solutions at 60 °C

	HCl:HF	HCl:NH_4FHF	HCl:H_3PO_4	HCl:H_2O
R (µm/h)	7.25	3	39	63
Ar	1.32	3.2	3.7	6.5

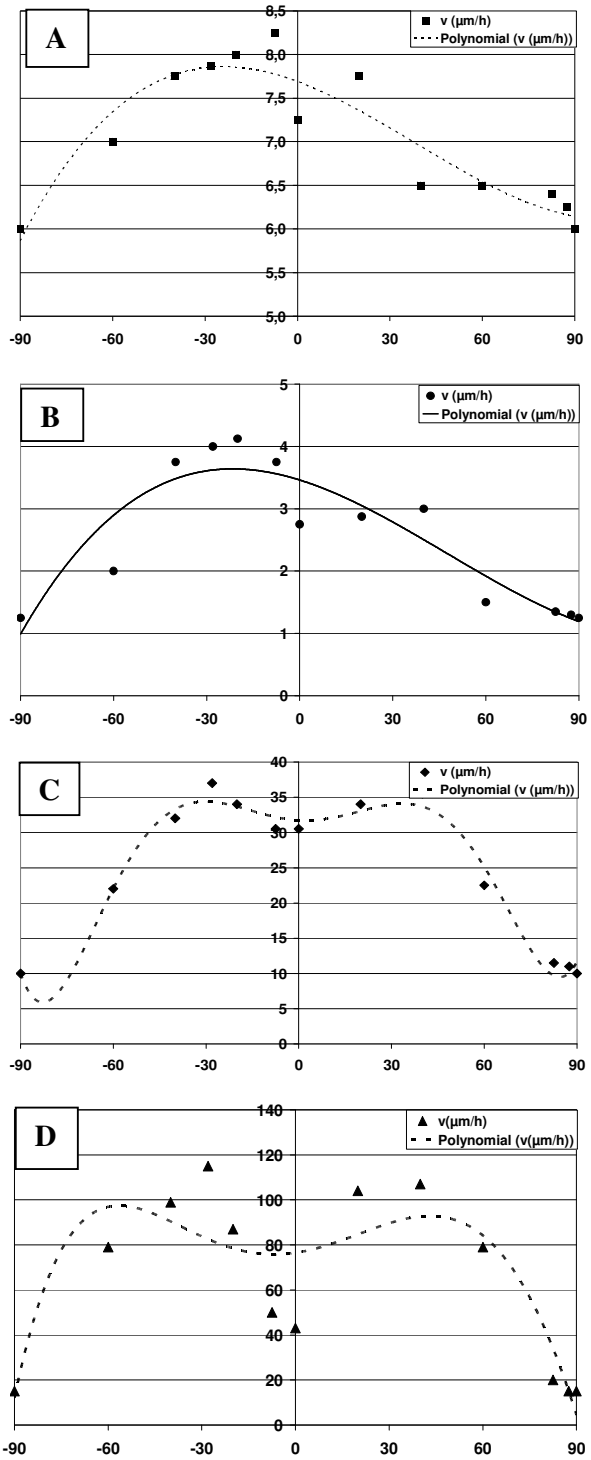

Fig.1 The etch rate versus the angle θ (°) in the case of HCl:HF (A), HCl:NH_4FHF (B), HCl:H_3PO_4 (C) and HCl:H_2O (D) etching at 60 °C.

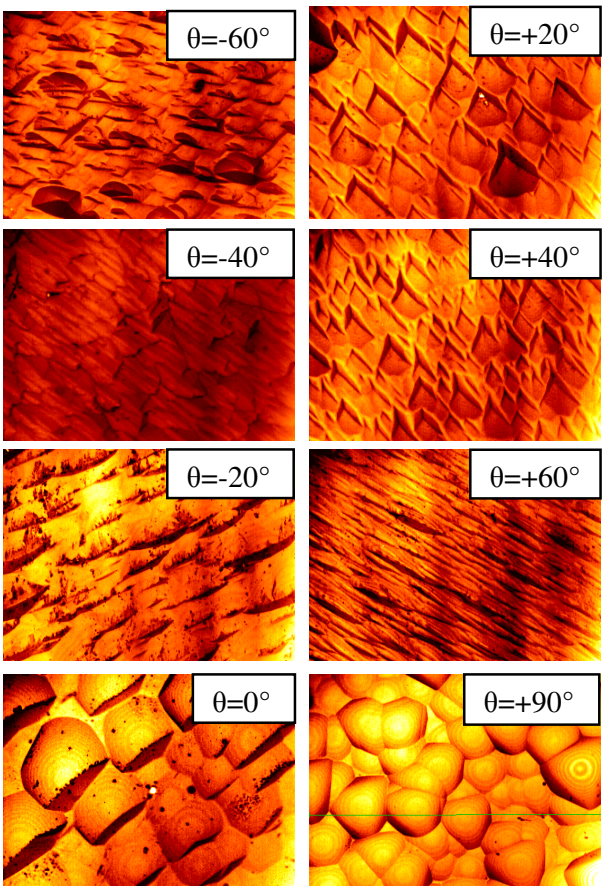

Fig.2 Surface texture of some Y± θ cuts etched in a H_3PO_4:HCl solution during 4 hours. The surface area is 125*95 μm^2

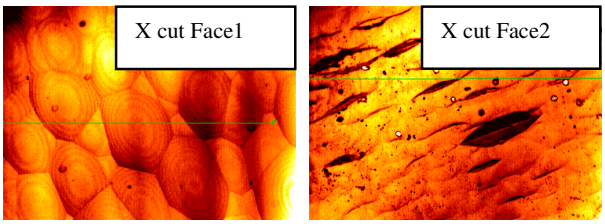

Fig. 3 Geometrical features of an X cut face 1 and face 2 etched in a HCl:H_3PO_4 solution

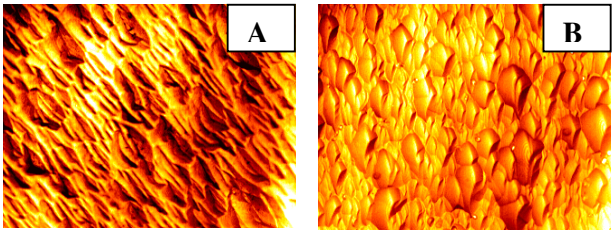

Fig. 4 Surface texture of an Y-60° plate after a prolonged etching in: HCl :HF (A) and HCl : NH_4FHF (B) solutions. These images were obtained using an interferometric microscope

It should be also remarked that the degradation of X cut face 2 is more marked than for face 1 in the HCl: H_3PO_4 solution (Table 4). After etching, face 1 seems as a polished surface. According to Fig.5, we can conclude that the HCl:H_2O solution provides average roughness criteria lower than the other etchant.

So, thanks to the previous results on the anisotropic factor, the dissolution rates and the surface roughness, the etching steps for producing 3D structures will be performed in the HCl:H_2O bath at 60°C.

MICROMACHINING OF RESONANT STRUCTURES

Experimental procedure

A thin square X plate (200µm thick) is coated by a double layer of SiO_2/Si_3N_4 using PECVD. A thermal aging of the double layer is carried at 400°C during 5 hours before the patterning of masks. On the mask are patterned rectangular shapes aligned along Y and Z directions. These shapes lead to the cantilevers. Two rectangles ending by a large square are used to obtain a tuning fork aligned along Y axis. A photolithographic process followed by an etching of 6 hours allowed the machining of several sizes of cantilevers.

Experimental results

The micromachined structure was investigated by SEM. Fig.6A shows a series of identical cantilevers. The mask pattern grooves between the beams vary from 50µm to 1000µm. All the beams shown on Fig.6A have been released but let us emphasize that the beams separated by a 50µm groove are not opened. A prolonged etching duration would allow the opening of the structure. The next image (Fig.6B) constitutes a magnification of the beams whose mask layers were separated by 200µm width. An underetch of 60µm (along the Z axis) is observed, as well as a 50° tilt facet at the built-in end of the beam from the wafer. A similar underetching develops along Z axis and the lateral shoulder is inclined of 45° to the surface of the wafer. We clearly depict the absence of concave undercut. Fig.6C exhibits the importance of convex undercutting at the end of a beam aligned along Z axis.

Fig.7 exhibits a tuning fork constituted by two beams whose pattern widths were 500µm. After 6 hours of etching, we measure a width of 380µm just under the mask which gives an underetch of 60µm; it's in agreement with the results obtained for the cantilevers. The beam width at mid thickness is 540µm. If we increase the etching duration (about 3 hours more), the lateral plane which bonds the beam will disappear to leave a vertical side.

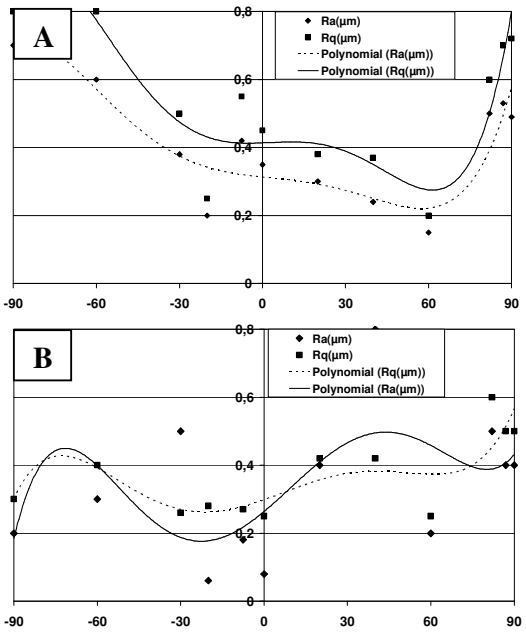

Fig.5 Roughness parameters Ra and Rq (µm) versus the angle θ.Case (A) HCl :H_3PO_4 solution, case (B) HCl : H_2O solution. These parameters were obtained after a 4h etching at 60°C.

Table 4. Roughness parameters for an X cut etched in HCl :H_2O or HCl : H_3PO_4 solution

X cut	HCl :H_2O		HCl : H_3PO_4	
	Ra (µm)	Rq (µm)	Ra (µm)	Rq (µm)
Face 1	0.35	0.5	0.09	0.14
Face 2	0.4	0.5	0.35	0.45

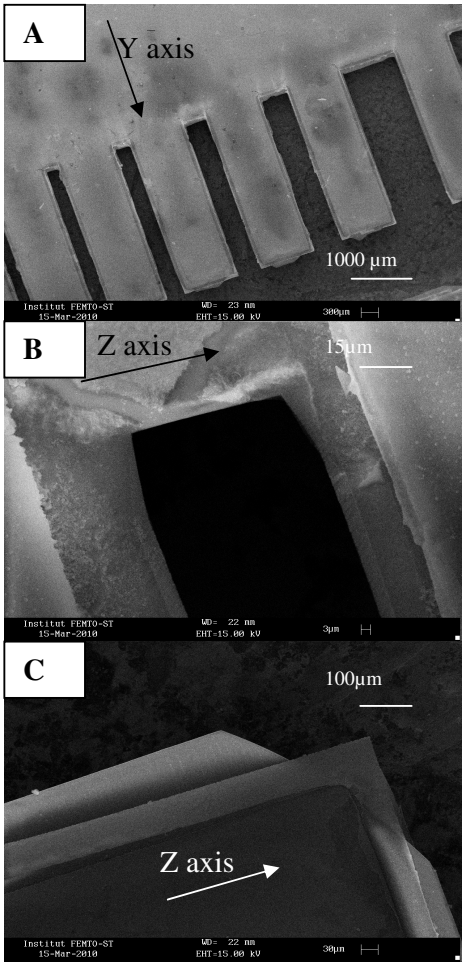

Fig. 6 SEM images of cantilevers etched on an X cut

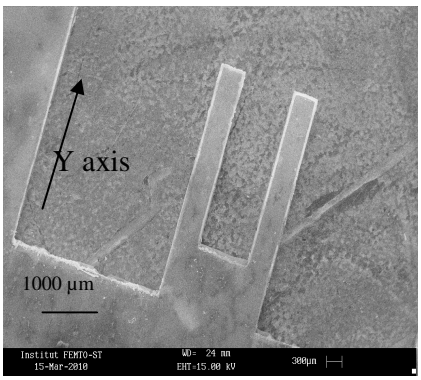

Fig. 7 SEM image of the turning fork aligned along Y axis

CONCLUSION

An exhaustive characterisation of the etch rates, the surface texture and the surface roughness after a prolonged etching in an HCl based solution was performed for langasite crystal. The best chemical etching conditions have been determined and a complete process has been developed for the micromachining in a $HCl:H_2O$ solution of cantilevers and tuning forks. The analysis of etching shapes has revealed a large underetching and convexe undercutting. The obtained etching data must be taken into account for the design of chemically etched langasite devices. Future works will be focus on the development of langasite vibrating inertial sensors, such as Vibrating Beam Accelerometer (VBA) and Coriolis Vibrating Gyro (CVG).

REFERENCES

[1] H. Fritze, H. L. Tuller, "Langasite for high temperature bulk acoustic wave applications", *Appl. Phys. Lett.* 78 (2001) 976-977

[2] Q. Kang, H.J. Zhang, X.Y. Liu and D.Z. Shen, "Oscillating frequency response of a langasite crystal microbalance in liquid phase*", Chin. Chem. Letters*, 16 (11) (2005) 1547-1550

[3] O. Le Traon, D. Janiaud, D. Pernice, S. Masson, S. Muller, J-Y. Tridera , "A New Quartz Monolithic Differential Vibrating Beam Accelerometer", *Proc. of the IEEE/ION Position*, Location And Navigation Symposium, San Diego, 24-27 april 2006.

[4] J. Guérard, M. Descharles, D. Janiaud, O. Le Traon, "Digital/Analog Electronic Architecture for Coriolis Vibrating Gyro", *Proc. of the Gyro Technology Symposium*, Karlsruhe, sept. 2009.

[5] O. Le Traon, S. Masson, C. Chartier, D. Janiaud, "LGS and GaPO4 Piezoelectric Crystals: New results", *Solid State Sci* (2009) doi1016/j.solidstatessciences.2009.06.032.

[6] E. Ansorge, S. Schimpf, S. Hirsch, J. Sauerwald, H. Fritze and B. Schmidt, "Piezoelectric driven resonant beam array in langasite", *Sensors and Actuators A* 132 (2006) 271-277

[7] G. Douchet, F. Sthal, T. Leblois, P. Vairac and E. Bigler, "Resonant LGS microsensor for scanning microdeformation microscopy", *Proc. IEEE Ultrasonics Symposium*, Sept. 2009, Rome, Italy, 4pp

[8] S. Laffey, M. Hendrickson, J. R. Vig, "Polishing and etching langasite and quartz crystals", *Proc. IEEE Int. Freq. Contr. Symp.* (1994) 245-250

[9] C. Tellier, M. Akil and T. Leblois, "A database for the etching of LGS in $H_2SO_4:H_2O$", *Proc. IEEE Int. Freq. Contr. Symp.* (2007) 671-677

[10] C. Tellier, M. Akil and T. Leblois, "Wet etching of LGS crystals in $H_3PO_4:H_20$", *Proc. IEEE Ultrasonics Symp.* (2006), Vancouver, Canada, 4pp

[11] ANSI/IEEE Std 176-1987, *IEEE Standards on piezoelectricity* (IEEE Inc., New York, 1987).